Supporting Information

Mirror-coupled plasmonic nanostructures for enhanced in-plane magnetic dipole emission

Ruizhao Yao, Sheng Lan, Guang-Can Li*

† Guangdong Provincial Key Laboratory of Nanophotonic Functional Materials and Devices, School of Information and Optoelectronic Science and Engineering, South China Normal University, 510006 Guangzhou, China. *e-mail: guangcan.li@m.scnu.edu.cn

1. Simulation configuration

The simulations in this study were performed with the three-dimensional finite- finite-element methods (FEM), implemented by the commercially available FEM solver (COMSOL Multiphysics). The dielectric constant of Ag was interpolated from experimental data (Ref. 44 in the main text). A two-step approach was used to calculate the scattering response. As illustrate in Fig. S1, first, the nanoparticles were set being absent, and a plane wave was injected from a top plane above the nanoparticles (450 nm away from the mirror). Then the plane wave source was disabled, and the background field calculated from the first step was used as the source to excite the simulation domain with the nanoparticles at present. The plane monitor hanging above collects the scattering light and was used to analysis the scattering responses. For dipole excitation, the plane wave source was disabled, and single electric or magnetic dipoles was positioned in the specific gaps to drive the nanoantennas. For simplicity, the nanoparticles were immersed in the air. The simulation domain was truncated by perfect matched layers (PMLs) to mimic the electromagnetic scattering or emission responses in infinite space. To ensure a robust iteration convergence in simulation, a mesh size of 1 nm and 0.2 nm were set for the nanoparticle volumes and the gap regions, respectively.

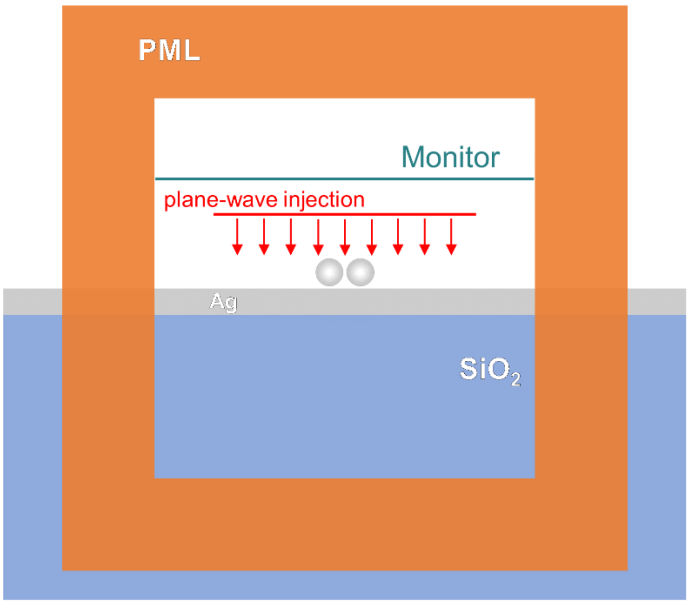

Figure S1. Schematic of numerical simulation configuration.

2. The field distributions at the resonant MD wavelength of single VNT4, VNT3 and VNT4' nanostructures.

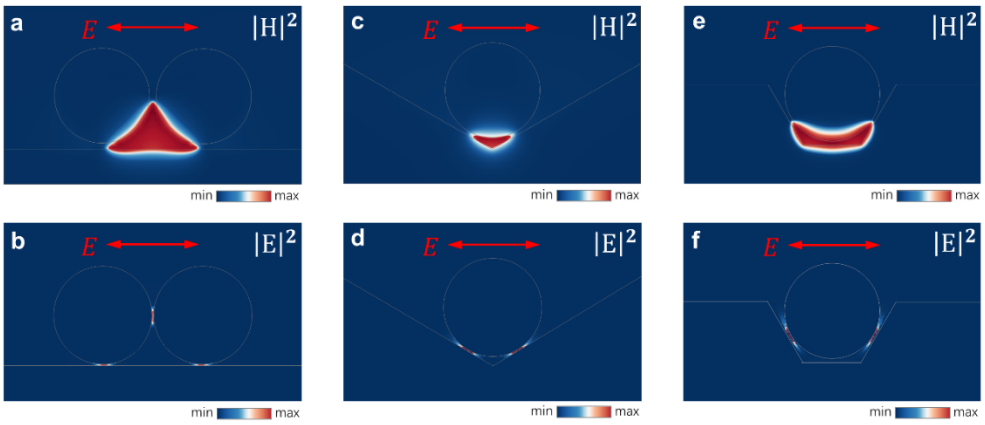

Figure S2. (a, b) The magnetic (a) and electric (b) intensity distributions calculated for single VNT4 structures at the resonant MD wavelength (720 nm). The arrow indicates the electric polarization of the excitation light, here a plane wave incident from the top. (c, d) Similar results as (a, b) but for a VNT3 structure. (e, f) Similar results as (a, b) but for a VNT4' structure. All the geometric parameters employed in the simulations are identical to that in Fig. 2 in the main text.

3. The intensity distributions of each magnetic field components at the MD resonance wavelength of single nanoantennas.

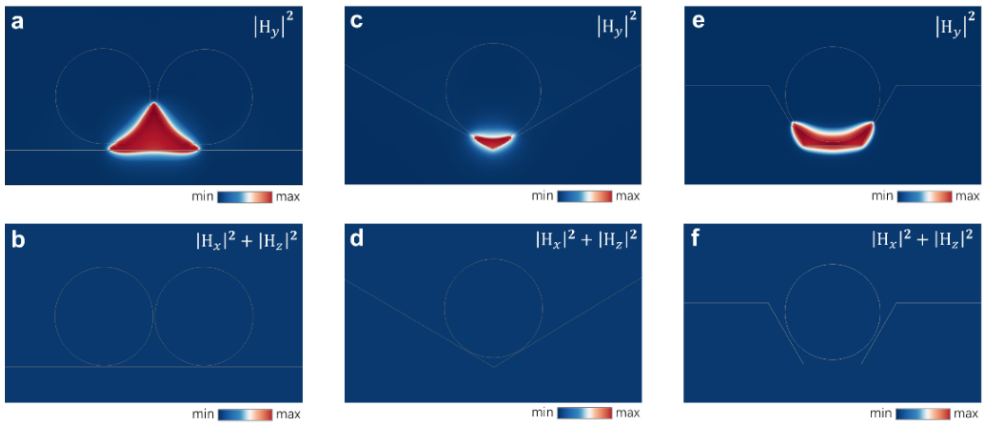

Figure S3. (a, b) The intensity distributions of each magnetic field components at the MD resonance wavelength of single VNT4 nanoantenna. (c, d) Similar results as (a, b) but for a VNT3 structure. (e, f) Similar results as (a, b) but for a VNT4' structure.

4. Scattering multipole responses of the magnetic nanoantennas illuminated by plane wave

We performed multipole expansion of the scattering response of the three nanoantennas. The results presented in Fig. S4a and b reveal the ED and MD mode of the VNT4 and VNT3 structures show nearly equal scattering strengths, and together dominate the total scattering responses. For the VNT4', the MD mode dominates the total scattering, though mixed with nonnegligible ED contribution (Fig. S4c). These observations are markedly different from the emission multipole expansion results of the dipole excitation cases showing solely MD-dominated radiation (Fig. 5 in the main text), suggesting the scattering multipole response of the nanoantennas depend strongly on the excitation conditions. Previous theoretical studies showed the presence of a metal substrate would induce significant electromagnetic coupling between the ED and MD modes [1], which leads to concurrent ED and MD excitations under plane wave illumination, making the MD mode not so pure magnetic. When excited by local MD (see Fig. 5) or ED (see Fig. 6) emitters properly positioned in the gaps, the scattering response could be more magnetic. Despite the ED-dressed MD scattering response, we should keep in mind the excitations at the MD wavelength are

dominantly driven by the magnetic field of illumination light (as demonstrated in Fig. 3), a key characteristic indicative of magnetic mode nature.

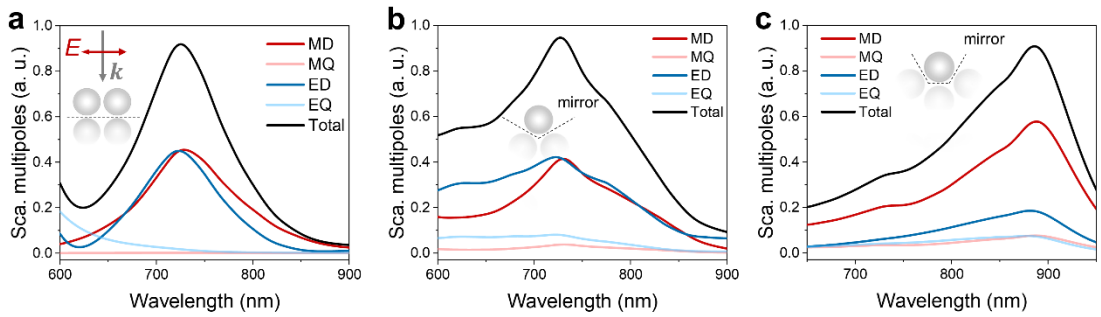

Figure S4. Multipole expansion of the scattering responses of single magnetic nanoantennas illuminated by plane wave. (a) Scattering multipoles of single VNT4 structure excited by plane wave polarized along the dimer axis (E_x). Inset shows the excitation configuration. (b) Same result as (a) but calculated for a VNT3 nanoantenna. (c) Same result as (a) but calculated for a VNT4' nanoantenna.

5. Multipole expansions of the scattering of single VNT4 with decreasing particle-film gap distances

For single VNT4 structures, shrinking the gap between the nanodimer and the underlying mirror leads to broadened line widths of the MD resonance (see Fig. 3). This can be attributed to intensified nanoparticle-mirror coupling at smaller gap distances, which not only intensify the MD strength, but also induces a significant ED mode component due to the so-called magnetoelectric coupling effect[1]. When narrowing the nanoparticle-mirror gap distances, the MD contribution to the total mode strength at the resonance wavelength increases and simultaneously, the contribution of the ED component decreases (see Fig. S5, S6). The significantly reduced ED contribution at thinner gap distances makes the narrowing effect induced by an ED resonance, which is well-known[2,3], marginally observable. In contrast, the stronger in-plane MD resonance gains enhanced strength when approaching a metal substrate, which consequently exhibit widen resonance linewidth[4],[1].

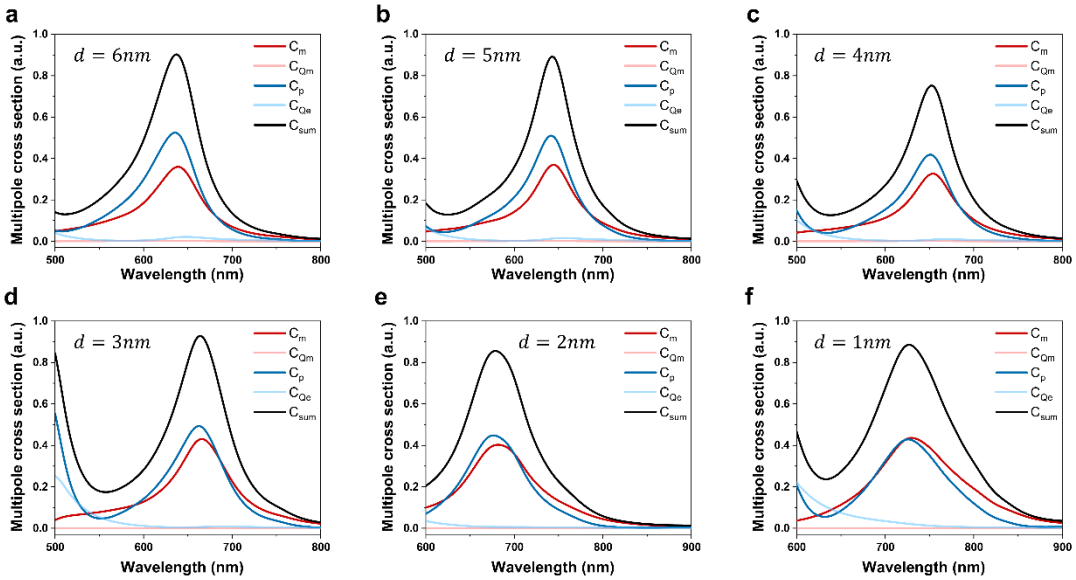

Figure S5 Multipolar expansion of the scattering response of single VNT4 structures with decreasing nanoparticle-mirror distances. C_m, C_p, C_{Qm}, C_{Qe} and C_{sum} correspond to the cross sections of magnetic dipole (MD), electric dipole (ED), magnetic quadrupole (MQ), electric quadrupole (EQ) and the total scattering, respectively.

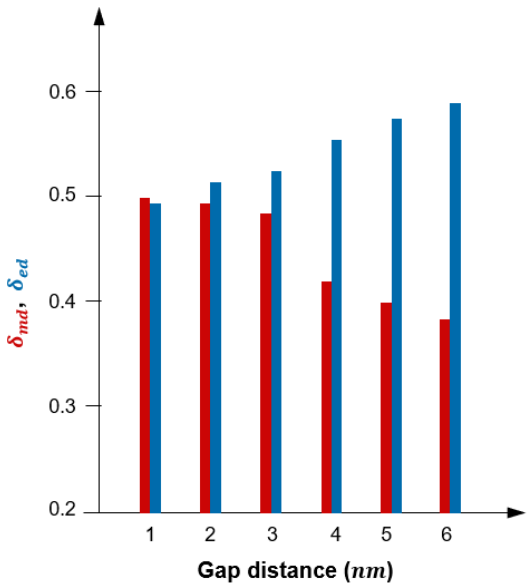

Figure S6. Evolution of the contribution weights of ED (δ_{ed}) and MD (δ_{md}) components to the total mode strength of a VNT4 nanoantenna with decreasing nanoparticle-mirror gap distances. The contribution weights of the multipole component are evaluated at the MD resonance wavelength (results extracted from Fig. S3).

6. Vanished magnetic resonances in nanoantennas with collapsed gaps.

The electron tunneling across narrow gaps would become significant nanoantenna structures with gaps smaller than 1 nm. Such quantum effect is not captured by the classical electromagnetic model used in the main text. Previous studies developed a quantum corrected model (QCM) to describe these tunneling events in a single nanoparticle dimer. This semi-analytical model predicted intensified electric shorting across the narrowing dimer gap, which eventually turns the capacitive bonding dipolar resonance into a conductive one when the two nanoparticles touch each other, i.e., charge transfer plasmon resonance (CTP). Here we're not going to employ the QCM model to numerically inspect the MD resonance evolution of single nanoantennas with decreasing gap distance below 1 nm. This is because, on one hand, such calculations gave rise to inconsistent results in previous studies[5–7], and on the other hand, without comparison with experimental results, it is hard to validate the QCM-based calculation results. Despite these, we can imagine that, with decreasing gap distance below 1 nm, the enhanced electric shorting due to intensified QT effects will weaken the magnetic dipole resonance of single gaped structures, which eventually leads to vanished MD resonance when the facing metal surfaces touch each other. In this regard, we can employ the classical electromagnetic model to evaluate the extreme case where the gap distances shrink to zero. The results are shown in Fig. S7. As can be seen, the MD resonance of single VNT4, VNT3 and VNT4' indeed vanish when the particle-mirror gap collapse (gap distance $d = 0$), in sharp contrast to their counterparts with $d = 1\ nm$, which show negligible quantum tunneling effects and significant MD resonances.

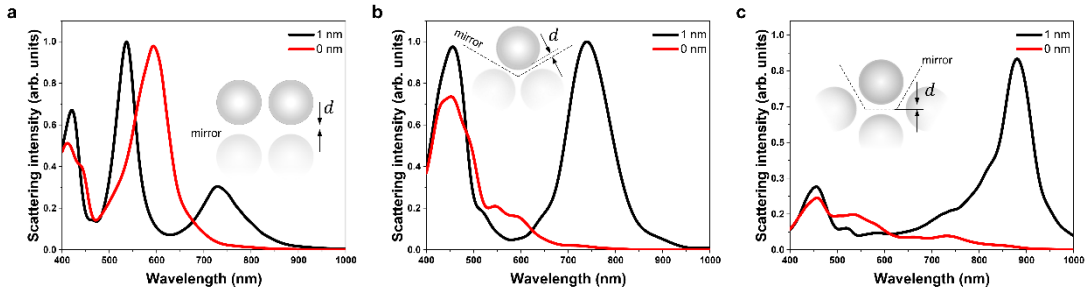

Figure S7. Vanished MD resonances in single magnetic nanoantenna structures. (a) The scattering spectra of single VNT4 structures with capacitive ($d = 1\ nm$,black) or conductive ($d = 0$, red)

coupling gaps. The excitation source is a pane wave incident from the top of the structures, with the electric polarization aligned with the dimer axis. (b) Similar results as (a) but for single VNT3 structure. (c) Similar results as (a) but for single VNT4' structure.

7. The nanocube dimer case

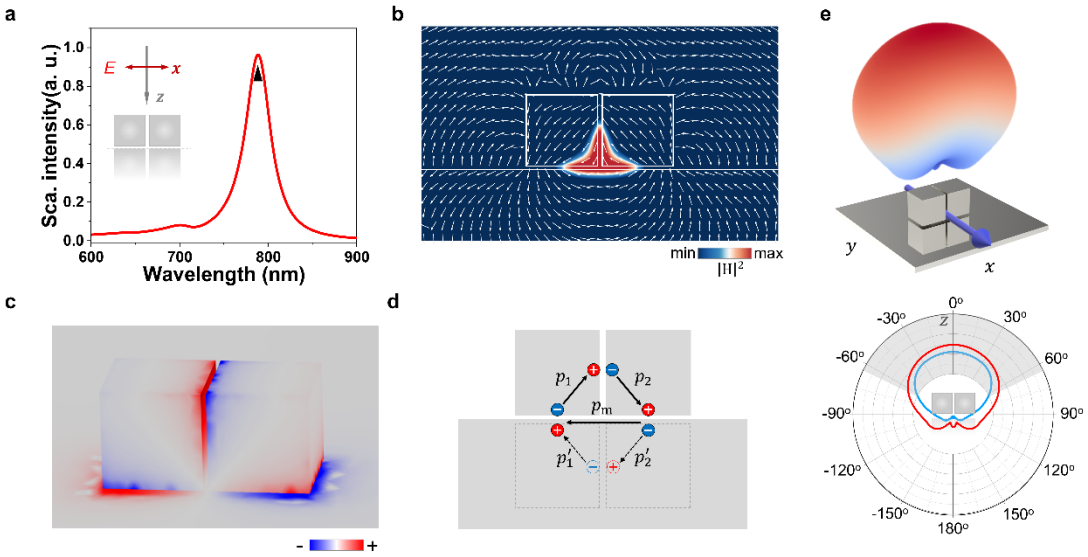

Figure S8. The magnetic response of an Ag nanocube dimer on mirror. (a) Simulated scattering spectrum of an Ag nanocube dimer on mirror illuminated by plane wave polarized along$x$. The length of the nanocube is 40 nm. The interparticle gap distance is 2 nm and the particle-mirror gap is 2 nm. (b, c) The magnetic field (b) and charge (c) distribution calculated at the plasmon resonance wavelength as marked in (a). (d) Schematic of the electric dipoles forming the magnetic dipole response, inferred from the charge distribution shown in (c). (e) Emission pattern of a magnetic dipole emitter positioned at the magnetic field hotspot (indicated in b), calculated at the plasmon resonance wavelength (marked in a). The emission profile of a pure magnetic dipole lying on the mirror (m_0) is also provided for reference (blue curve).

8. Determination of the mode origin of single Nanoparticle-on-mirror (NPoM) structures.

The single VNT3 nanostructures evolves into a NPoM structure when the angle between two supporting mirrors is 180°. In this configuration, we can still observe strong confinement of magnetic fields inside the gap area (Fig. S9a). However, this

resonance is not necessarily a magnetic mode, as evidenced by the calculated surface charge distributions at the resonance wavelength (Fig. S9b), which indicates a typical electric dipole mode yet damped by the underlying mirror. This complex resonance, to some extent, can be viewed as an electric quadrupole mode with broken symmetry. To further confirm its electric origin, we scan a single NPoM nanostructure through a tightly focused Gaussian beam and inspect its site-dependent absorption intensities (as illustrated in Fig. S9c). At the resonance wavelength, the absorption profiles of the single NPoM perfectly follow the electric field distributions along the scanning path, other than the magnetic field component (Fig. S9d). This means the single NPoM nanostructure dominantly responds to the electric field of light, a characteristic indicative of an electric-type mode.

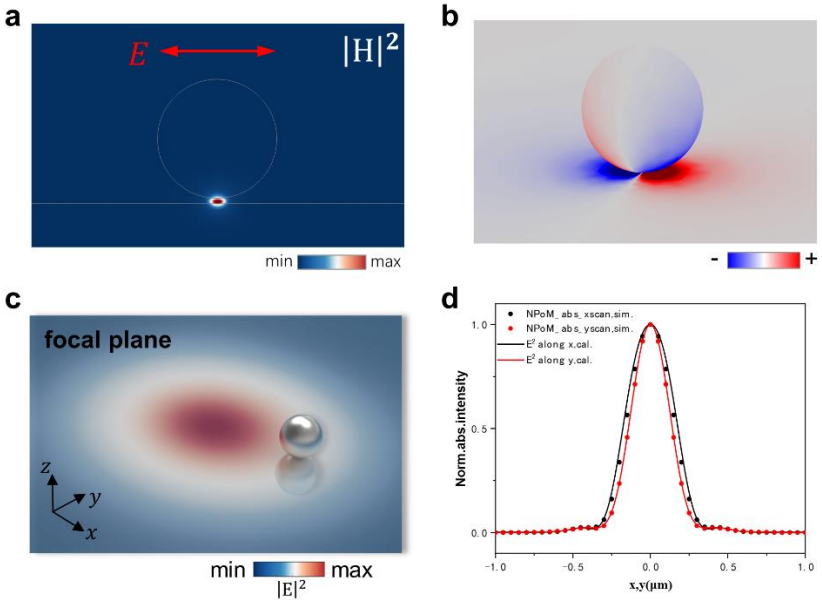

Figure S9. The electromagnetic properties of single nanoparticle-on-mirror (NPoM) structures. (a) The magnetic field distributions of a NPoM structure, calculated at the resonance wavelength. (b) correlated surface charge distribution with that in (a). (c) schematical illustration of a NPoM structure scanning through a focused Gaussian beam. (d) Site-dependent absorption profile of a NPoM and the electric field distributions along the scanning paths.

9. The collection efficiency of an out-of-plane MD source in free space

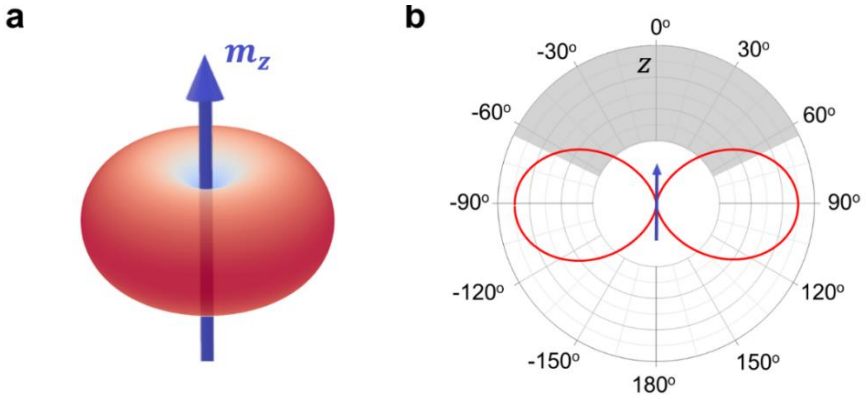

Figure S10. (a) The radiation pattern of a vertically aligned magnetic dipole (m_z). (b) The polar plotting of the radiation pattern in (a). the shadowed region corresponds to the collection angle of a microscope objective with NA=0.9.

10. Mapping the focused azimuthally polaized beam

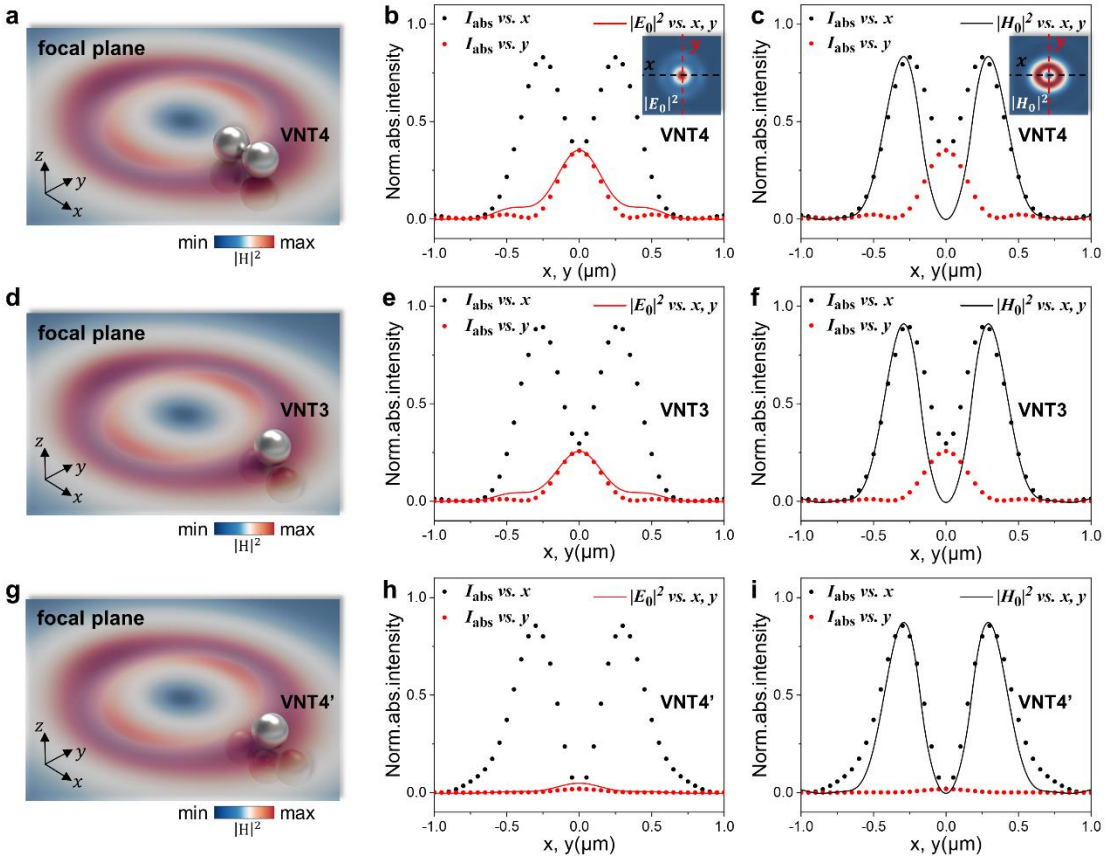

Figure S11. Excitation responses of single MD nanostructures. (a) Schematics of single VNT4

nanoantenna scanning through a focused azimuthally polarized (AP) beam. The rendered backgrounds represent the magnetic field distributions in the focal plane of a focused AP beam. The numerical aperture (NA) of the focusing lens is 0.9. (b) Comparison of the absorption intensities vs. x, y (dots) and the focal electric ($|E_0|^2$) intensities vs. x, y (solid line), calculated for single VNT4 scanning along the x or y axis. Inset shows the electric field distribution at the beam focus. These scanning absorption profiles are simulated at the resonant wavelengths as marked in Fig. 2 (black triangles). (c) Comparison of the VNT4 absorption intensities vs. x, y (dots) and the focal magnetic ($|H_0|^2$) intensities vs. x, y (solid line). Inset shows the electric field distribution in the focal plane. (d-f) Similar results as (a-c) but calculated for a VNT3 scanning through the same AP beam. (g-i) Similar results as (a-c) but calculated for a VNT4' scanning through the same beam focus.

11. Comparison of the far-field radiation responses between a real nanoparticle tetramer, VNT4-coupled MD source, and an in-plane MD source atop a mirror.

The virtual ring-shaped nano-oligomers shown in the main text have similar topological geometry configurations as their real counterparts. So, we can expect similar magnetic responses previously observed for the real ones and now in the virtual ones. For example, the single virtual nanotetramer formed from a dimer-on-mirror architecture shows spectral characters much like that of a real nanotetramer in air, both featuring a pronounced magnetic plasmon resonance in the visible to near-infrared region (Fig. S12) and strong magnetic field confinement in the center structural gaps. However, their emission patterns may be quite different because of the presence of the infinitely large mirror substrate in the virtual nano-tetramers. As shown in Fig. S13, the emission of a real nano-tetramer in air exhibits the well-known doughnut-shaped profile, same as that of an ideal magnetic dipole source. For the virtual nano-tetramer, despite the magnetic resonances originated from the tetramer configuration formed from the dimer and the image dipoles, their emissions are strongly reflected by the infinitely large mirror to the upper space and interfere with the direct emission, resulting in the balloon-like emission patterns as shown in Fig. S13b. This mirror effect can be confirmed by a comparison to the mirror-modified

emission of an ideal magnetic dipole source. As shown in Fig S13b and c, the emission of a virtual nano-oligomer highly resembles to that of an ideal atop a mirror. We anticipate similar effects are ubiquitous in other particle-on-mirror structures with resonant magnetic response originated form a virtual ring-shaped oligomer configuration.

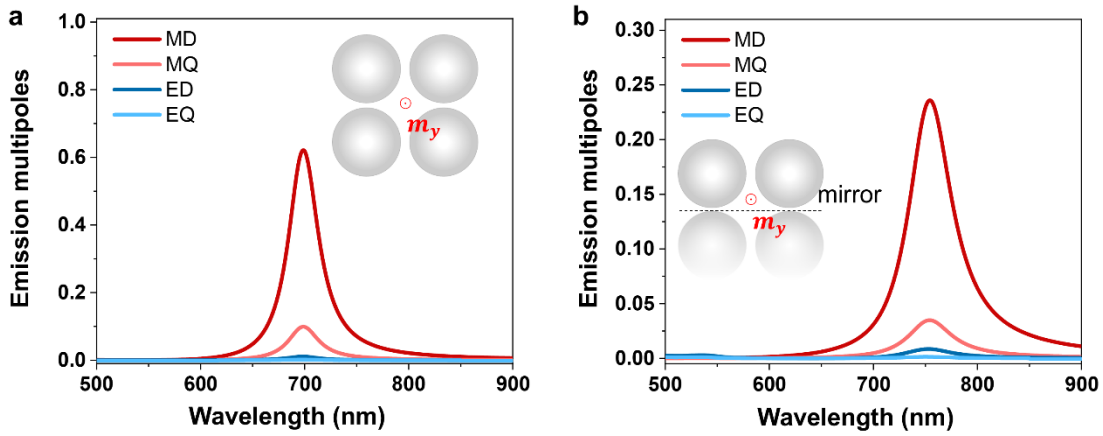

Figure S12. Comparison of the emission spectra of a real nanotetramer in air (a) and a virtual nanotetramer formed from a dimer-on-mirror structure (b), both excited by a magnetic dipole source located at the center gap of the structures (see insets). The nanoparticle sizes are set of the same for both the real (a) and virtual (b) nano-tetramers.

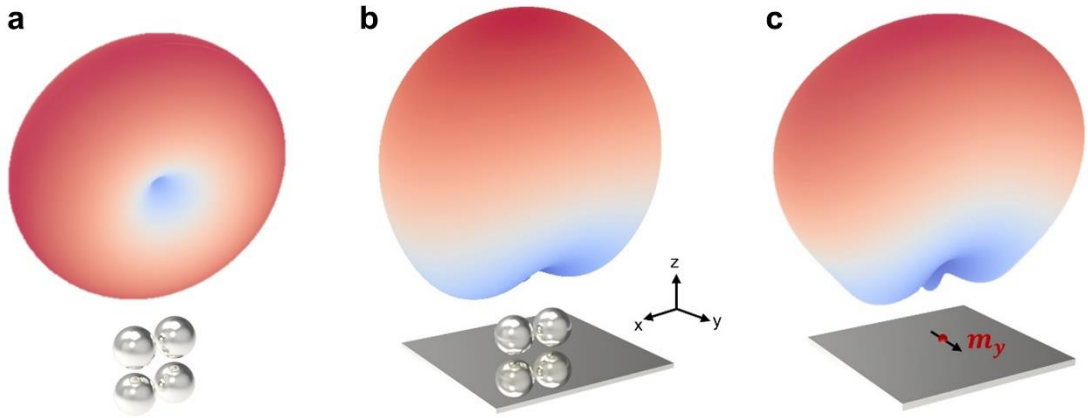

Figure S13. The emission patterns calculated for a MD source (m_y) respectively coupled to a real nanotetramer (a), a VNT4 antenna formed from the dimer-on-mirror structure (b) and a mirror (c). In a and b, the dipole is in the center gap of the structures (as shown in Fig. S12). The dipole-mirror distance in c is 1 nm.

References

[1] A. E. Miroshnichenko, A. B. Evlyukhin, Y. S. Kivshar, B. N. Chichkov, *ACS Photonics* **2015**, *2*, 1423.

[2] G. C. Li, Y. L. Zhang, J. Jiang, Y. Luo, D. Y. Lei, *ACS Nano* **2017**, *11*, 3067.

[3] A. Sobhani, A. Manjavacas, Y. Cao, M. J. McClain, F. J. García De Abajo, P. Nordlander, N. J. Halas, *Nano Lett* **2015**, *15*, 6946.

[4] I. Sinev, I. Iorsh, A. Bogdanov, D. Permyakov, F. Komissarenko, I. Mukhin, A. Samusev, V. Valuckas, A. I. Kuznetsov, B. S. Luk'yanchuk, A. E. Miroshnichenko, Y. S. Kivshar, *Laser Photon Rev* **2016**, *10*, 799.

[5] J. Jose, L. Schumacher, M. Jalali, G. Haberfehlner, J. T. Svejda, D. Erni, S. Schlücker, *ACS Nano* **2022**, *16*, 21377.

[6] K. J. Savage, M. M. Hawkeye, R. Esteban, A. G. Borisov, J. Aizpurua, J. J. Baumberg, *Nature* **2012**, *491*, 574.

[7] W. Zhu, R. Esteban, A. G. Borisov, J. J. Baumberg, P. Nordlander, H. J. Lezec, J. Aizpurua, K. B. Crozier, *Nature Communications* **2016**, *7*, 11495.